PHYSICAL REVIEW D VOLUME 24, NUMBER 7 1 OCTOBER 1981

Large-angle two-photon exclusive channels in quantum chromodynamics

Stanley J. Brodsky
Stanford Linear Accelerator Center,
Stanford University, Stanford, California 94305

G. Peter Lepage
Laboratory of Nuclear Studies,
Cornell University, Ithaca, New York 14853
(Received 1 June 1981)

Detailed leading-order quantum-chromodynamics (QCD) predictions are given for the scaling, angular, and helicity dependence of the reactions $\gamma\gamma\to M\bar{M}$ ($M=\pi$, K, ρ, etc.) at large momentum transfer. In addition to providing a basic test of QCD at short distances, measurements can be used to determine the process-independent meson distribution amplitudes $\phi_M(x,Q)$. Other related two-photon channels such as $\gamma\gamma\to\gamma\rho$, $\gamma^*\gamma\to\pi^0,\eta^0,\eta'$, and $\eta_c\to\gamma\gamma$ are also discussed. We also prove the existence of a fixed Regge singularity at $J=0$ which couples to $\gamma\rho\to\gamma\rho$ in the t channel but not to $\gamma\pi\to\gamma\pi$.

I. INTRODUCTION

Much effort has recently been devoted to the study of exclusive processes involving large transverse momenta within the context of perturbative quantum chromodynamics (QCD).[1,2] Here, as in other applications of perturbative QCD, photon-induced reactions play an important role. The pointlike structure of the photon results in substantial simplifications of the analysis of these exclusive scattering amplitudes. In this paper we present detailed predictions for photon-photon annihilation into two mesons at large center-of-mass angles $\theta_{\text{c.m.}}$. We also examine predictions for photon-meson transition form factors, and for a number of other two-photon processes relevant to the study of perturbative QCD.

Amplitudes for the large-angle exclusive processes discussed here factor into two parts at high energies[1]: (1) a parton distribution amplitude $\phi(x_i,Q)$ for each hadron—the probability amplitude for finding valence partons in the hadron, each carrying some fraction x_i of the hadron's momentum, and all collinear up to $k_{\perp i}\sim Q$, the typical momentum transferred in the process; and (2) a hard-scattering amplitude T_H—the amplitude for scattering the clusters of collinear valence partons from each hadron. Thus, for example, the process $\gamma_\lambda\gamma_{\lambda'}\to\pi\pi$ is described by the helicity amplitudes [see Fig. 1(a)]

$$\mathcal{M}_{\lambda\lambda'}(s,\theta_{\text{c.m.}})=\int_0^1 dx\,dy\,\phi_\pi^*(x,\tilde{Q}_x)\phi_\pi^*(y,\tilde{Q}_y)\times T_{\lambda\lambda'}(x,y;s,\theta_{\text{c.m.}})\,, \tag{1}$$

where $\tilde{Q}_x\sim\min(x,1-x)\sqrt{s}\,|\sin\theta_{\text{c.m.}}|$, and similarly for $\tilde{Q}_y$. The quark distribution amplitudes depend only logarithmically on s, having the form

$$\phi_\pi(x,Q)=x(1-x)\sum_{n=0}^{\infty}a_n^{(\pi)}C_n^{3/2}(1-2x)\left[\ln\frac{Q^2}{\Lambda^2}\right]^{-\gamma_n} \tag{2}$$

to leading order in $\alpha_s(Q^2)$, the running coupling constant in QCD. The hard-scattering amplitude $T_{\lambda\lambda'}$ is computed, in leading order, from Born diagrams such as those in Fig. 1(b). All quark and hadron masses may be neglected in these diagrams, resulting in errors only of order $m^2/s\ll 1$. Consequently, simple dimensional analysis implies $T_{\lambda\lambda'}\sim\alpha_s/s$ for large s and, therefore,

$$\mathcal{M}_{\lambda\lambda'}\to\frac{1}{s}f(\theta_{\text{c.m.}},\varphi),\quad s\to\infty\,,$$

up to factors of $(\ln s/\Lambda^2)$. Furthermore, in vector-gluon theories like QCD, quark helicity is conserved along each fermion line when masses are neglected. Thus the meson helicities in $\gamma\gamma\to\rho\rho$, for example, must be equal and opposite, to leading order in m^2/s. This is not the case in scalar- or tensor-gluon theories.[3]

Dimensional counting[4] and hadronic helicity conservation are general features of the wide-angle exclusive processes which we consider here.[5] They are valid to all orders in α_s, and as such are important tests of the theory, testing the scale invariance of the bare couplings, the vector nature of the gluon, and so on. However, we can say much more about these photon-induced reactions at large momentum transfer. Specifically, we give detailed predictions for the magnitude, angular distribution, and helicity structure of these amplitudes.[3] Furthermore, we can use these processes to probe the nonperturbative structure of the hadronic wave functions.

In Sec. II, we discuss two-photon annihilation into two mesons. This analysis is combined with that of the meson's electromagnetic form factor so as to remove many of the ambiguities due to renormalization scheme, normalization point, and so on, which usually beset such a QCD calculation. We also discuss the power-law-suppressed contributions due to vector dominance and Landshoff pinch singularities. In Sec. III, we examine the photon-meson transition form factor at large Q^2 (for $e\gamma\to eM$ at wide angles) and its relation to the pion form factor. We also show how current-algebra predictions for low Q^2 can be combined with QCD predictions for high Q^2 to obtain a rough prediction for $F_{\gamma M}(Q^2)$ for all Q^2. In Sec. IV we review predictions for a number of other two-photon processes. Finally, in Sec. V, we summarize our results and briefly discuss some of their broader implications.

II. PHOTON-PHOTON ANNIHILATION INTO TWO MESONS

In this section we examine the two-photon processes $\gamma_\lambda\gamma_{\lambda'}\to M_h\bar{M}_{h'}$ where $M_h, M_{h'}$ are mesons with helicities h and h', respectively. Dimensional counting predicts that for large s, $s^4(d\sigma/dt)$ scales at fixed t/s or $\theta_{\text{c.m.}}$ up to factors of $\ln(s/\Lambda^2)$, for all such reactions. Hadronic-helicity conservation requires that either both meson helicities are zero, or both are equal to ±1, with $h=-h'$. (There is no *a priori* restriction on the photon helicities.) We discuss these two cases separately.

A. Helicity-zero mesons

Some 40 diagrams contribute to the hard-scattering amplitudes for $\gamma\gamma\to M\bar{M}$ (for nonsinglet mesons). These can be derived from the four independent diagrams in Fig. 1(b) by particle interchange. The resulting amplitudes for helicity-zero mesons are

$$\left.\begin{matrix}T_{++}\\T_{--}\end{matrix}\right\}=\frac{16\pi\alpha_s}{3s}\frac{32\pi\alpha}{x(1-x)y(1-y)}\left[\frac{(e_1-e_2)^2a}{1-\cos^2\theta_{\text{c.m.}}}\right], \tag{3}$$

$$\left.\begin{matrix}T_{+-}\\T_{-+}\end{matrix}\right\}=\frac{16\pi\alpha_s}{3s}\frac{32\pi\alpha}{x(1-x)y(1-y)}\left[\frac{(e_1-e_2)^2(1-a)}{1-\cos^2\theta_{\text{c.m.}}}+\frac{e_1e_2a[y(1-y)+x(1-x)]}{a^2-b^2\cos^2\theta_{\text{c.m.}}}\right]+\frac{(e_1^2-e_2^2)(x-y)}{2}\Bigg],$$

where

$$\left.\begin{matrix}a\\b\end{matrix}\right\}=(1-x)(1-y)\pm xy\ ,$$

the subscripts $++, --, \cdots$ refer to photon helicities, and e_1, e_2 are the quark charges [i.e., the mesons have charges $\pm(e_1-e_2)$]. To compute the $\gamma\gamma\to M\bar{M}$ amplitude $\mathcal{M}_{\lambda\lambda'}$ [Eq. (1)], we now need only know the x dependence of the meson's distribution amplitude $\phi_M(x,\tilde{Q})$; the overall normalization of ϕ_M is fixed by the "sum rule" ($n_c=3$):

$$\int_0^1 dx\,\phi_M(x,Q)=\frac{f_M}{2\sqrt{3}}\ , \tag{4}$$

where f_M is the meson decay constant as determined from leptonic decays.[6] Note that the dependence in x and y of several terms in $T_{\lambda\lambda'}$ is quite similar to that appearing in the meson's electromagnetic form factor.

$$F_M(s)=\frac{16\pi\alpha_s}{3s}\int_0^1 dx\,dy\frac{\phi_M^*(x,\tilde{Q}_x)\phi_M^*(y,\tilde{Q}_y)}{x(1-x)y(1-y)} \tag{5}$$

when $\phi_M(x,Q)=\phi_M(1-x,Q)$ is assumed.[7] Thus much of the dependence on $\phi(x,Q)$ can be removed from $\mathcal{M}_{\lambda\lambda'}$ by expressing it in terms of the meson form factor—i.e.,

$$\left.\begin{matrix}\mathcal{M}_{++}\\ \mathcal{M}_{--}\end{matrix}\right\}=16\pi\alpha F_M(s)\left[\frac{\langle(e_1-e_2)^2\rangle}{1-\cos^2\theta_{\text{c.m.}}}\right],$$

$$\left.\begin{matrix}\mathcal{M}_{+-}\\ \mathcal{M}_{-+}\end{matrix}\right\}=16\pi\alpha F_M(s)\left[\frac{\langle(e_1-e_2)^2\rangle}{1-\cos^2\theta_{\text{c.m.}}}+2\langle e_1e_2\rangle g[\theta_{\text{c.m.}};\phi_M]\right], \tag{6}$$

up to corrections of order α_s and m^2/s. Now the only dependence on ϕ_M, and indeed the only unknown quantity, is in the θ-dependent factor

$$g[\theta_{\text{c.m.}};\phi_M]=\frac{\int_0^1 dx\,dy\frac{\phi_M^*(x,\tilde{Q})\phi_M^*(y,\tilde{Q})}{x(1-x)y(1-y)}\frac{a[y(1-y)+x(1-x)]}{a^2-b^2\cos^2\theta_{\text{c.m.}}}}{\int_0^1 dx\,dy\frac{\phi_M^*(x,\tilde{Q})\phi_M^*(y,\tilde{Q})}{x(1-x)y(1-y)}}. \tag{7}$$

The spin-averaged cross section follows immediately from these expressions

$$\begin{aligned}\frac{d\sigma}{dt}&=\frac{2}{s}\frac{d\sigma}{d\cos\theta_{\text{c.m.}}}=\frac{1}{16\pi s^2}\frac{1}{4}\sum_{\lambda\lambda'}|\mathcal{M}_{\lambda\lambda'}|^2\\&=16\pi\alpha^2\left|\frac{F_M(s)}{s}\right|^2\left\{\frac{\langle(e_1-e_2)^2\rangle^2}{(1-\cos^2\theta_{\text{c.m.}})^2}+\frac{2\langle e_1e_2\rangle\langle(e_1-e_2)^2\rangle}{1-\cos^2\theta_{\text{c.m.}}}g[\theta_{\text{c.m.}};\phi_M]\right.\\&\qquad\left.+2\langle e_1e_2\rangle^2g^2[\theta_{\text{c.m.}};\phi_M]\right\}.\end{aligned} \tag{8}$$

In Figs. 2 and 3, $g[\theta_{\text{c.m.}};\phi_M]$ and the spin-averaged cross section (for $\gamma\gamma\to\pi\pi$) are plotted for several forms of $\phi_M(x,Q)$. At very large energies, the distribution amplitude evolves to the form

$$\phi_M(x,Q)\underset{Q\to\infty}{\to}\sqrt{3}f_Mx(1-x), \tag{9}$$

and the predictions [curve (a)] become exact and parameter free. However, this evolution with increasing Q^2 is very slow (logarithmic), and at current energies ϕ_M could be quite different in structure, depending upon the details of hadronic binding. Curves (b) and (c) correspond to the extreme examples $\phi_M\propto[x(1-x)]^{1/4}$ and $\phi_M\propto\delta(x-\frac{1}{2})$, respectively. Remarkably, the cross section for charged mesons is essentially independent of the choice of ϕ_M, making this an essentially parameter-free prediction of perturbative QCD. By contrast, the predictions for neutral helicity-zero mesons are quite sensitive to the structure of ϕ_M. Thus we can study the x dependence of the meson distribution amplitude by measuring the angular dependence of this process.

The cross sections shown in Fig. 3 are specifically for $\gamma\gamma\to\pi\pi$, where the pion form factor has been

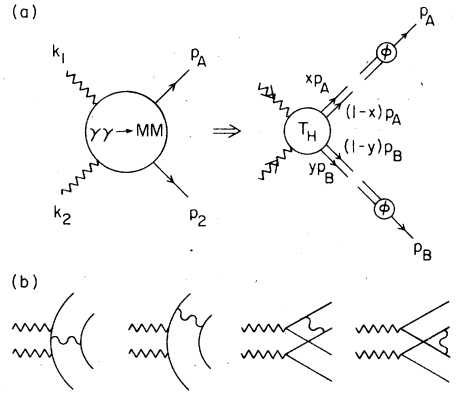

FIG. 1. (a) Factorized structure of the $\gamma\gamma\to M\bar{M}$ amplitude in QCD at large momentum transfer. The T_H amplitude is computed with quarks collinear with the outgoing mesons. (b) Diagram contributing to T_H ($\gamma\gamma\to M\bar{M}$) to lowest order in α_s.

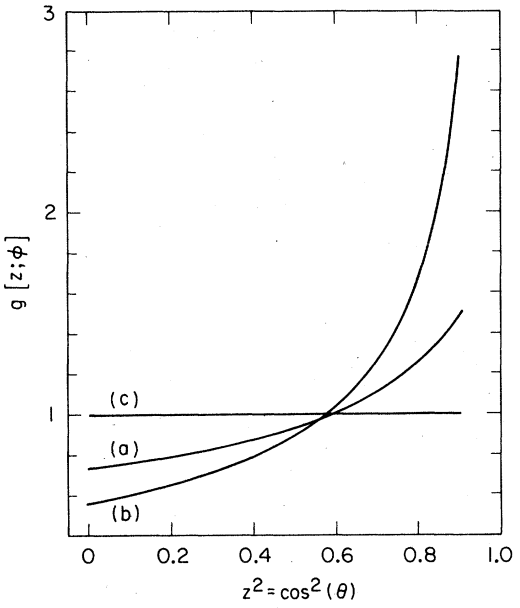

FIG. 2. The θ-dependent factor $g[\cos\theta_{\text{c.m.}};\phi_M]$ of Eq. (7) required for computing the $\gamma\gamma\to M\bar{M}$ amplitude for helicity-zero mesons. The curves (a), (b), and (c) correspond to the distribution amplitudes $\phi_M(x,Q)$ $\propto x(1-x)$, $[x(1-x)]^{1/4}$, and $\delta(x-\frac{1}{2})$, respectively.

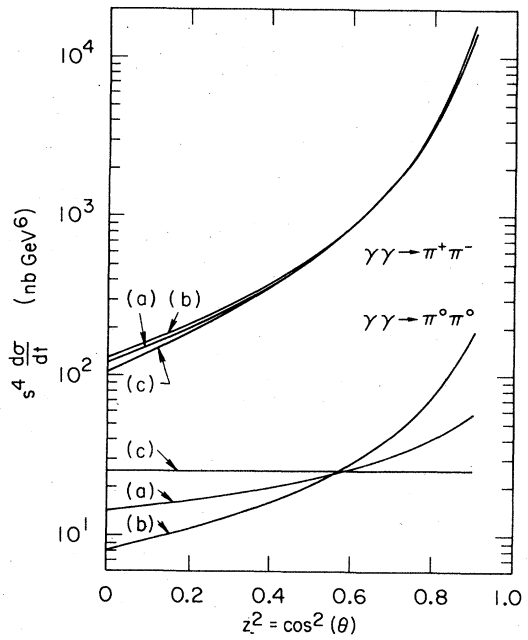

FIG. 3. QCD predictions for $\gamma\gamma\to\pi\pi$ to leading order in QCD. The results assume the pion-form-factor parametrization $F_\pi(s)\sim 0.4\ \text{GeV}^2/s$. Curves (a), (b), and (c) correspond to the distribution amplitudes ϕ_M $=x(1-x)$, $[x(1-x)]^{1/4}$, and $\delta(x-\frac{1}{2})$, respectively. Predictions for other helicity-zero mesons are obtained by multiplying with the scale constants given in Table I.

approximated by $F_\pi(s)\sim 0.4\ \text{GeV}^2/s$. The $\pi^+\pi^-$ cross section is quite large at moderate s:

$$\frac{\frac{d\sigma}{dt}(\gamma\gamma\to\pi^+\pi^-)}{\frac{d\sigma}{dt}(\gamma\gamma\to\mu^+\mu^-)}\sim\frac{4|F_\pi(s)|^2}{1-\cos^4\theta_{\text{c.m.}}}$$

$$\sim\frac{0.6\ \text{GeV}^4}{s^2}\quad\text{at }\theta_{\text{c.m.}}=\frac{\pi}{2}\ . \tag{10}$$

Similar predictions are possible for other helicity-zero mesons. The normalization of $\gamma\gamma\to M\bar{M}$ relative to the $\gamma\gamma\to\pi\pi$ cross section is completely determined by the ratio of meson decay constants $(f_M/f_\pi)^4$ and by the flavor symmetry of the wave functions, provided only that ϕ_M and ϕ_π are similar in shape. Given this assumption, we obtain the all-orders (in α_s) relations presented in Table I. Note that the cross section for charged ρ's with helicity zero is almost an order of magnitude larger than that for charged π's [Eq. (10)]. Cross sections involving the η' have been omitted. Flavor-singlet pseudoscalar mesons, like the η', have a two-gluon valence Fock state which contributes to leading order. These will be discussed elsewhere.[8]

Finally, notice that the leading-order predictions [Eq. (6)] have no explicit dependence on α_s. Thus they are relatively insensitive to the choice of a renormalization scheme or of a normalization scale. This is not the case for either the form factor or the two-photon annihilation amplitude when examined separately. However, by combining the two analyses as in Eq. (6), we obtain meaningful results without computing $O(\alpha_s)$ corrections.

B. Helicity-one mesons

Again the diagrams of Fig. 1(b) determine the hard-scattering amplitudes which describe the production of helicity ±1 ("transversely" polarized) mesons in $\gamma\gamma$ annihilation. The resulting helicity amplitudes for $\gamma\gamma\to M\bar{M}$ are

$$\mathcal{M}_{++,-+}=\mathcal{M}_{++,+-}=\mathcal{M}_{--,+-}=\mathcal{M}_{--,-+}=0\ ,$$

$$\left.\begin{matrix}\mathcal{M}_{+-,+-}\\ \mathcal{M}_{-+,-+}\end{matrix}\right\}=16\pi\alpha F_{M_\perp}(s)\{\langle(e_1-e_2)^2\rangle+2\langle e_1e_2\rangle\cos\theta_{\text{c.m.}}(1-\cos\theta_{\text{c.m.}})g_\perp[\theta_{\text{c.m.}};\phi_{M_\perp}]\}\ , \tag{11}$$

$$\left.\begin{matrix}\mathcal{M}_{+-,-+}\\ \mathcal{M}_{-+,+-}\end{matrix}\right\}=16\pi\alpha F_{M_\perp}(s)\{\langle(e_1-e_2)^2\rangle-2\langle e_1e_2\rangle\cos\theta_{\text{c.m.}}(1+\cos\theta_{\text{c.m.}})g_\perp[\theta_{\text{c.m.}};\phi_{M_\perp}]\}\ ,$$

where we define (in analogy to the helicity-zero case) a "transverse form factor"

$$F_{M_\perp}(s)\equiv\frac{16}{3}\frac{\pi\alpha_s}{s}\int_0^1 dx\,dy\frac{\phi^*_{M_\perp}(x,\tilde{Q}_x)\phi^*_{M_\perp}(y,\tilde{Q}_y)}{x(1-x)y(1-y)}\ , \tag{12}$$

and where

$$g_\perp[\theta_{\text{c.m.}};\phi_{M_\perp}]\equiv\frac{\displaystyle\int_0^1 dx\,dy\,\frac{\phi^*_{M_\perp}(x,\tilde{Q}_x)\phi^*_{M_\perp}(y,\tilde{Q}_y)}{x(1-x)y(1-y)}\frac{b^2}{a^2-b^2\cos^2\theta_{\text{c.m.}}}}{\displaystyle\int_0^1 dx\,dy\,\frac{\phi^*_{M_\perp}(x,\tilde{Q}_x)\phi^*_{M_\perp}(y,\tilde{Q}_y)}{x(1-x)y(1-y)}}\ . \tag{13}$$

Of course hadronic-helicity conservation (in QCD) implies $\mathcal{M}_{\lambda\lambda',++}=\mathcal{M}_{\lambda\lambda',--}=0$ as well—i.e., 12 out of the 16 helicity amplitudes vanish in leading order (in QCD). The spin-averaged cross section can now be written

$$\frac{d\sigma}{dt}(\gamma\gamma\to M_\perp\bar{M}_\perp)=16\pi\alpha^2\left|\frac{F_{M_\perp}(s)}{s}\right|^2\{\langle(e_1-e_2)^2\rangle^2-4\langle e_1e_2\rangle\langle(e_1-e_2)^2\rangle\cos^2\theta_{\text{c.m.}}g_\perp[\theta_{\text{c.m.}};\phi_{M_\perp}]$$
$$+2\langle e_1e_2\rangle^2\cos^2\theta_{\text{c.m.}}(1+\cos^2\theta_{\text{c.m.}})g_\perp^2[\theta_{\text{c.m.}};\phi_{M_\perp}]\}\ . \tag{14}$$

In Fig. 4, $g_\perp[\theta_{\text{c.m.}};\phi_{M_\perp}]$ is plotted for the three *Ansätze* for $\phi_{M_\perp}$ used in the previous section. Hadronic-helicity conservation implies that only helicity-zero mesons can couple to a single highly virtual photon. So $F_{M_\perp}$, the transverse form factor, cannot be directly measured experimentally. Here we will *assume* that the longitudinal and transverse form factors are equal so as to obtain a rough estimate of the $\gamma\gamma\to\rho_\perp\rho_\perp$ cross section (Fig. 5).[9] Again we see strong dependence on $\phi_{M_\perp}$ for all angles except $\theta_{\text{c.m.}}\sim\pi/2$, where the terms involving $g_\perp$ vanish. Consequently, a measurement of the angular distribution would be very sensitive to the x dependence of $\phi_{M_\perp}$, while measurements at $\theta_{\text{c.m.}}=\pi/2$ determine $F_M(s)$. Notice also that the number of charged ρ pairs (with any helicity) is much larger than the number of neutral ρ's, particularly near $\theta_{\text{c.m.}}=\pi/2$. The cross sections are again quite large with

$$\left.\frac{\frac{d\sigma}{dt}(\gamma\gamma\to\rho_\perp^+\rho_\perp^-)}{\frac{d\sigma}{dt}(\gamma\gamma\to\mu^+\mu^-)}\right|_{\theta_{\text{c.m.}}=\pi/2}\sim\frac{5\ \text{GeV}^4}{s^2}\ . \tag{15}$$

Results for the $\omega_\perp$ and $\phi_\perp$ are given in Table I.

C. Nonleading processes: Vector dominance; pinch singularities

The QCD predictions given here for wide-angle $\gamma\gamma\to M\bar{M}$ processes are in marked contrast to those which are expected from vector dominance (VD) of on-shell photon interactions. Dimensional counting implies that contributions from the minimal Fock state of a hadron (i.e., $|q\bar{q}\rangle$ of mesons, $|qqq\rangle$ for baryons) always dominate at high energies and large angles. The scattering amplitude is suppressed by an extra power of $1/\sqrt{s}$ for each additional parton involved in the hard subprocess

TABLE I. Wide-angle high-energy relations for $\gamma\gamma$ annihilation into two helicity 0 ($h=0$) or helicity ±1 ($h=\pm1$) mesons. Here η-η' mixing is neglected and probably $f_\eta \sim f_\pi = 93$ MeV. The ϕ is assumed to have only strange quarks in its valence Fock state.

	Process	Cross section
$h=0$	$\gamma\gamma \to K^+K^-$	$2\frac{d\sigma}{dt}(\gamma\gamma\to\pi^+\pi^-)$
	K_LK_S	$0.3\frac{d\sigma}{dt}(\gamma\gamma\to\pi^0\pi^0)$
	$\pi\eta$	$0.1\left[\frac{f_\eta}{f_\pi}\right]^2\frac{d\sigma}{dt}(\gamma\gamma\to\pi^0\pi^0)$
	$\eta\eta$	$0.4\left[\frac{f_\eta}{f_\pi}\right]^4\frac{d\sigma}{dt}(\gamma\gamma\to\pi^0\pi^0)$
	$\gamma\gamma\to\rho^+\rho^-$	$7.5\frac{d\sigma}{dt}(\gamma\gamma\to\pi^+\pi^-)$
	$\rho^0\rho^0$	$7.5\frac{d\sigma}{dt}(\gamma\gamma\to\pi^0\pi^0)$
	$\rho^0\omega$	$3\frac{d\sigma}{dt}(\gamma\gamma\to\pi^0\pi^0)$
	$\omega\omega$	$8\frac{d\sigma}{dt}(\gamma\gamma\to\pi^0\pi^0)$
	$\phi\phi$	$1.4\frac{d\sigma}{dt}(\gamma\gamma\to\pi^0\pi^0)$
$h=\pm1$	$\gamma\gamma\to\rho^0\omega$	$0.4\frac{d\sigma}{dt}(\gamma\gamma\to\rho^0\rho^0)$
	$\omega\omega$	$\frac{d\sigma}{dt}(\gamma\gamma\to\rho^0\rho^0)$
	$\phi\phi$	$0.2\frac{d\sigma}{dt}(\gamma\gamma\to\rho^0\rho^0)$

(i.e., T_H). Since the photon is an elementary field, its minimal Fock state is just the bare photon itself; the photon couples directly into T_H for leading subprocesses. On the other hand, vector dominance is associated with the $|q\bar{q}\rangle$ Fock state of the photon. This Fock state is analyzed in the same way any strongly interacting meson is analyzed: the photon is replaced by a collinear, on-shell q-$\bar{q}$ pair in T_H; T_H is convoluted with the photon's quark distribution amplitude $\phi_\gamma(x,\tilde{Q})$. If ρ dominance is assumed, ϕ_γ is proportional to ϕ_ρ and the $\gamma\gamma\to M\bar{M}$ amplitude due just to the photon's $|q\bar{q}\rangle$ component, is proportional to $\rho^0\rho^0\to M\bar{M}$. Several features distinguish these contributions from the leading terms described above.

(1) The amplitude $\mathcal{M}^{\rm VD}(\gamma\gamma\to M\bar{M})$ due to vector dominance is suppressed by an additional power of $1/s$ for large s and $\theta_{\rm c.m.}$. This follows directly from dimensional counting.

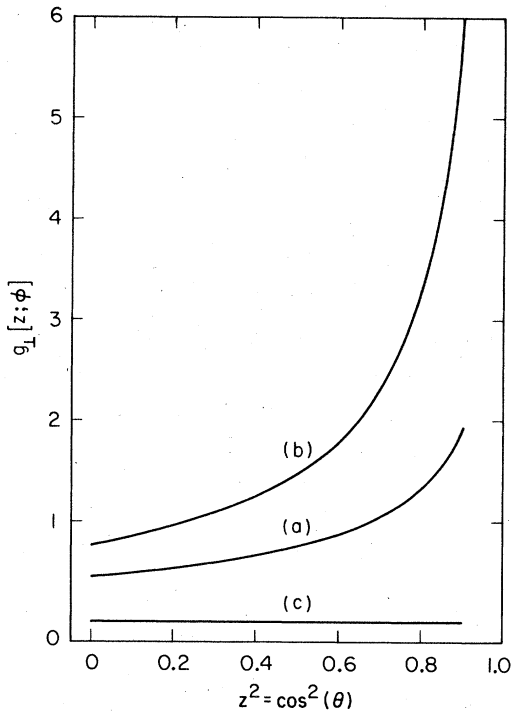

FIG. 4. The factor $g_\perp[\cos\theta_{\rm c.m.};\phi_M]$ of Eq. (7) required for computing the $\gamma\gamma\to M\bar{M}$ amplitude for helicity ±1 mesons. See Fig. 2.

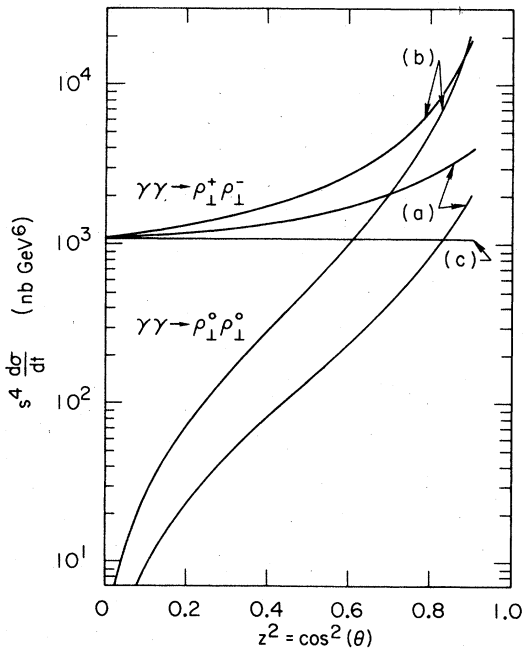

FIG. 5. QCD predictions for $\gamma\gamma\to\rho_\perp\bar{\rho}_\perp$ with opposite helicity ±1 to leading order in QCD. The normalization given here assumes that the ρ distribution amplitude is helicity independent. Other vector-meson results are obtained from the scale constants given in Table I.

(2) Hadronic-helicity conservation in QCD (for zero quark mass) requires that the sum of the photon helicities equal the sum of meson helicities for $\mathcal{M}^{\rm VD}$. Thus in contrast with Eq. (6), $\mathcal{M}^{\rm VD}_{++}$ and $\mathcal{M}^{\rm VD}_{--}$ vanish relative to $\mathcal{M}^{\rm VD}_{+-}$ for $\gamma\gamma\to\pi\pi$, KK, ... If just one of the photons couples through its $|q\bar{q}\rangle$ state, then all the reactions considered above are forbidden in leading order, leaving only $\gamma\gamma\to\rho_\perp\rho_\perp$, $\rho_\perp\pi$, and so on.

(3) The vector-dominated amplitudes have pinch singularities, resulting when each constitutent from one photon is paired with one from the other photon, and the two pairs scatter independently of one another. In lowest order this gives an amplitude which is suppressed by only $1/\sqrt{s}$ relative to the leading QCD term. However, radiative corrections, i.e., Sudakov form-factor effects, tend to further suppress these pinch contributions by about $1/\sqrt{s}$.[5]

We thus predict that the vector-dominated amplitudes for photon-induced reactions are unimportant at high energies and wide angles. The possibility still exists that they may play some role at moderate energies. However, data[10] for the closely related process $\gamma p\to\gamma p$ shows no sign of vector dominance for $s\gtrsim 5$ GeV^2, and $\theta_{\rm c.m.}\sim\pi/2$.

We emphasize that pinch singularities are suppressed in $\gamma\gamma\to M\bar{M}$ processes by at least $1/\sqrt{s}$ even for amplitudes in which the photon couples directly. The pinch singularity can only arise if the quark and antiquark coupling to the photon are collinear and near mass shell, in which case the analysis and results are analogous to those for $\rho\rho\to M\bar{M}$. The pinch contributions are further suppressed by radiative corrections; a leading-logarithm analysis results in a correction to the leading amplitude which is suppressed almost a full power of s.[5] This power-law suppression of pinch singularities, which is a special feature of photon-induced reactions, greatly simplifies the analysis and interpretation of these hadronic scattering amplitudes.

III. MESON-PHOTON TRANSITION FORM FACTORS

The photon-meson transition form factor $F_{M\gamma}(Q^2)$ can be measured using two-photon events in which one photon is far off the mass shell (with $q^2=-Q^2$). This is just the exclusive limit of the photon structure function (i.e., $e\gamma\to e\pi$) or fragmentation function (i.e., $e\bar{e}\to\gamma\pi$). Only neutral pseudoscalar mesons couple, and the $\gamma^*\gamma M$ vertex has the form

$$\Gamma_\mu=-ie^2F_{M\gamma}(Q^2)\epsilon_{\mu\nu\rho\sigma}P_M^\nu\epsilon^\rho q^\sigma\ ,$$

where P_M is the meson's momentum and ϵ^ρ the polarization vector of the initial (on-shell) photon. A complete analysis of this form factor for large Q^2 has been given in Ref. 1. For pions, the final result is [$\tilde{Q}=\min(x,1-x)Q$]

$$F_{\pi\gamma}(Q^2)=\frac{2}{\sqrt{3}Q^2}\int_0^1 dx\frac{\phi_\pi^*(x,\tilde{Q})}{x(1-x)}\left[1+O\left[\alpha_s,\frac{m^2}{Q^2}\right]\right] \tag{16}$$

Unlike the electromagnetic form factor $F_\pi(Q^2)$ [Eq. (5)], this form factor in leading order has no explicit dependence on $\alpha_s(Q^2)$. Consequently an accurate measurement of $F_{\pi\gamma}(Q^2)$ determines $\int_0^1 dx[\phi_\pi^*(x,\tilde{Q})/x(1-x)]$. This can be combined with the normalizing sum rule [Eq. (4)] to constrain the x dependence of $\phi_\pi(x,\tilde{Q})$. To illustrate this, consider normalized distribution amplitudes of the general form

$$\phi_\pi(x,\tilde{Q})=\frac{f_\pi}{2\sqrt{3}}\frac{\Gamma(2\eta+2)}{[\Gamma(\eta+1)]^2}(1-x)^\eta x^\eta,\quad \eta>0\ , \tag{17}$$

where large $\eta(\tilde{Q})$ implies a sharply peaked (at $x=\frac{1}{2}$) distribution and small $\eta(\tilde{Q})$ gives a broad distribution. This *Ansatz* gives a $\pi\gamma$ transition form factor

$$Q^2F_{\pi\gamma}(Q^2)=2f_\pi\frac{2\eta+1}{3\eta}\ , \tag{18}$$

which is clearly quite sensitive to the parameter η (see Fig. 6). For very high Q^2, $\eta(Q)\to 1$ and thus,

$$F_{\pi\gamma}\to\frac{2f_\pi}{Q^2}\ \text{ as } Q^2\to\infty\ . \tag{19}$$

The x dependence of the integrand in Eq. (16) is identical to that in Eq. (5) for $F_\pi(Q^2)$. Consequently all dependence on ϕ_π can be removed by comparing the two processes. In fact, a measurement of each provides a direct determination of $\alpha_s(Q^2)$[1]:

$$\alpha_s(Q^2)=\frac{1}{4\pi}\frac{F_\pi(Q^2)}{Q^2|F_{\pi\gamma}(Q^2)|^2}+O(\alpha_s^2)\ . \tag{20}$$

Once the $O(\alpha_s^2)$ corrections have been computed,[15] this could be used to measure α_s and the QCD scale parameter Λ for a given renormalization

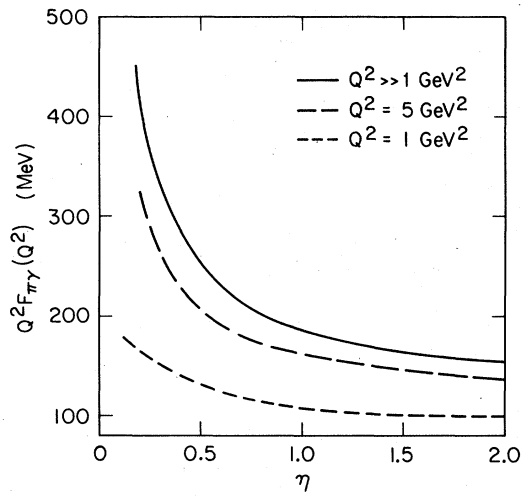

FIG. 6. Dependence of the $\gamma^*\gamma\to\pi$ transition form factor $F_{\pi\gamma}(Q^2)$ on the parametrization of the pion distribution amplitude given in Eq. (17).

prescription.

Of course, all of these formulas are valid only at large Q^2; $O(m^2/Q^2)$ corrections become important at lower Q^2. However, the $Q^2\to 0$ behavior of $F_{\pi\gamma}$ is fixed by the experimental rates for the decay $\pi^0\to 2\gamma$, or, equivalently as it turns out, by current algebra which implies[11]

$$F_{\pi\gamma}(Q^2)\to\frac{1}{4\pi^2 f_\pi} \quad \text{as } Q^2\to 0 . \tag{21}$$

To estimate the effects due to $O(m^2/Q^2)$ corrections, we write $F_{\pi\gamma}$ in terms of a monopole form

$$F_{\pi\gamma}\sim\frac{1}{4\pi^2 f_\pi}\frac{1}{1+(Q^2/8\pi^2 f_\pi{}^2)} \sim\frac{0.27\ \text{GeV}^{-1}}{1+Q^2/M^2} \quad (M^2\sim 0.68\ \text{GeV}^2) , \tag{22}$$

which interpolates between the $Q^2=0$ and $Q^2=\infty$ limits [Eqs. (21) and (19)]. The mass scale M^2 is quite similar to that measured for $F_\pi(Q^2)$. If the best $\eta(Q)$ in Eq. (17) is appreciably different from $\eta=1$ at current Q^2, this mass-scale parameter might actually be more like

$$M^2(\eta)=(0.68\ \text{GeV}^2)\frac{2\eta+1}{3\eta} . \tag{23}$$

Curves for $Q^2F_{\pi\gamma}(Q^2)$ which include such η-dependent mass effects are also given in Fig. 6. Mass corrections do not greatly alter the predictions for $Q^2\gtrsim 5$ GeV^2.

Similar predictions can be derived for $F_{\eta\gamma}$ and $F_{\eta'\gamma}$. If the π, η, and η' distribution amplitudes are all similar in shape, then we have

$$F_{\eta\gamma}(Q^2)=\frac{1}{\sqrt{3}}\frac{f_\eta}{f_\pi}F_{\pi\gamma}(Q^2) ,$$
$$F_{\eta'\gamma}(Q^2)=\left[\frac{2}{3}\right]^{1/2}\frac{f_{\eta'}}{f_\pi}F_{\pi\gamma}(Q^2) , \tag{24}$$

to all orders in α_s and to leading order in m^2/Q^2. Presumably the decay constants f_π, f_η, and $f_{\eta'}$ are all roughly equal. The gluonic valence state in the η' does not contribute in leading order to this process.

IV. OTHER PROCESSES

Other two-photon processes which can be analyzed perturbatively in QCD include the following.

(a) $\gamma\gamma\to p\bar{p},n\bar{n},\ldots$. The analysis for baryon-antibaryon final states is closely analogous to that for mesons, except that in general there are many more subprocesses contributing to T_H.[12] Dimensional counting predicts $s^6(d\sigma/dt)$ scaling up to logarithmic factors, and hadronic-helicity conservation implies that the baryons have equal and opposite helicities. We note that data exist for both the proton's Compton amplitude ($\gamma p\to\gamma p$) and for its magnetic form factor.[1,10] A detailed comparison with $\gamma\gamma\to p\bar{p}$ will provide new insights into the nucleon wave function. The Compton amplitude is $d\sigma/dt\sim 0.1$ nb/GeV^2 at $s\sim 9$ GeV^2 and $\theta=\pi/2$, suggesting that $\gamma\gamma\to p\bar{p}$ may be comparable with $\gamma\gamma\to\rho\rho,\pi\pi,\ldots$ for $s\lesssim 10$ GeV^2 and $\theta\sim\pi/2$.

(b) $\gamma\gamma\to\eta_c,\eta_b,\ldots$. One of the classic applications of two-photon physics is to the study of even-charge-conjugation mesons. Particularly interesting are the heavy-quark pseudoscalar mesons such as the η_c. As is well known, the leading $\eta_c\gamma\gamma$ coupling can be decomposed into a nonrelativistic wave function (evaluated at $\vec{r}=0$) multiplying a perturbative amplitude for $c\bar{c}\to\gamma\gamma$. This factorization is valid, subject to very general assumptions, to lowest and first order in $\alpha_s(M_{\eta_c}{}^2)$, and until nonperturbative bound-state effects of $O(v^2/c^2)$ become important. The total hadronic width of the η_c is analyzed in a similar fashion, proceeding via $\eta_c\to 2$ gluons in lowest order. Because the lowest-order amplitudes for two-photon and two-gluon decay are identical (up to overall color factors), the ratio of these widths is an especially clean prediction of perturbative QCD. All dependence on the wave function cancels, as do all

$O(v^2/c^2)$ corrections, to give (in the $\overline{\text{MS}}$ scheme)[13]

$$\frac{\Gamma(\eta_c \to \text{hadrons})}{\Gamma(\eta_c \to \gamma\gamma)} = \frac{2}{9}\frac{\alpha_s^2(M_{\eta_c}^2)}{\alpha^2}\frac{1}{(e_c)^4}\left[1+\frac{14\alpha_s(M_{\eta_c}^2)}{\pi}+\cdots\right]. \tag{25}$$

Thus a precise measurement of this ratio, for either the η_c or the η_b, determines the QCD scale parameter Λ. This must agree with that obtained from $\Gamma(\Upsilon \to \text{hadrons})/\Gamma(\Upsilon \to \mu^+\mu^-)$ or other short-distance processes. Quantities, such as this one, which are proportional to $(\alpha_s)^n$ will probably be the most useful for determining the parameters of QCD. In contrast, measuring small deviations from the scaling behavior predicted by naive parton models is difficult; interpreting these deviations is equally challenging due to higher-twist effects.

(c) $\gamma\gamma \to \gamma\rho$ Dimensional counting predicts $s^3(d\sigma/dt)$ scaling (up to logarithms) for $\gamma\gamma \to \gamma\rho$ at fixed $\theta_{\text{c.m.}}$. However, in QCD hadronic-helicity conservation requires that the ρ have zero helicity, which is impossible, when its mass is neglected, if it is coupled to the photons in a gauge-invariant and Lorentz-covariant fashion. Thus QCD requires additional suppression by a factor of $O(m^2/s)$, and $s^4(d\sigma/dt)$ scaling is more likely. This is *not* necessarily the case for theories with scalar or tensor gluons. These do not conserve hadronic helicity and so $s^3(d\sigma/dt)$ scaling may result.

V. SUMMARY AND CONCLUSIONS

As we have discussed in this paper, two-photon exclusive channels at large momentum transfer provide a particularly important laboratory for testing QCD since the large-momentum-transfer scaling behavior, helicity structure, and often even the absolute normalization can be rigorously computed for each channel. The $\gamma\gamma \to M\bar{M}$ and $\gamma^*\gamma \to M$ processes provide detailed checks of the basic Born structure of QCD, the scaling behavior of the quark and gluon propagators and interactions, as well as the constituent charges and spins. Conversely, the angular dependence of the $\gamma\gamma \to M\bar{M}$ amplitudes can be used to determine the shape of the process-independent distribution amplitude $\phi_M(x,Q)$ for valence quarks in the meson $q\bar{q}$ Fock state. The $\cos\theta_{\text{c.m.}}$ dependence of the $\gamma\gamma \to M\bar{M}$ amplitude determines the light-cone x dependence of the meson distribution amplitude in much the same way that the x_{Bj} (Bjorken x) dependence of deep-inelastic cross sections determines the light-cone x dependence of the structure functions (quark probability functions) $G_{q/M}(x,Q)$.

The form of the predictions given here are exact to leading order in $\alpha_s(Q^2)$. Power-law $(m/Q)^2$ corrections can arise from mass insertions, higher Fock states, pinch singularities, and nonperturbative effects. In particular, the predictions are only valid when s-channel resonance effects can be neglected. It is likely that the background due to resonances can be reduced relative to the leading-order QCD contributions if one measures the two-photon processes with at least one of the photons tagged at moderate spacelike momentum q^2, since resonance contributions are expected to be strongly damped by form-factor effects. In contrast, the leading-order QCD $\gamma_1\gamma_2 \to M\bar{M}$ amplitudes are relatively insensitive to the value of q_1^2 or q_2^2 for $|q_i^2| \ll s$.

Finally, we note that the amplitudes given in this paper have simple crossing properties. In particular, we can immediately analyze the Compton amplitude $\gamma M \to \gamma M$ in the region t large with $s \gg |t|$ in order to study the leading Regge behavior in the large-momentum-transfer domain. In the case of helicity ± 1 mesons, the leading contribution to the Compton amplitude has the form $(s \gg |t|)$

$$\mathcal{M}_{\gamma M \to \gamma M} = 16\pi\alpha F_{M_\perp}(t)(e_1^2+e_2^2) \qquad (\lambda_\gamma = \lambda'_\gamma,\ \lambda_M = \lambda'_M), \tag{26}$$

which corresponds to a fixed Regge singularity at $J=0$.[14] In the case of helicity-zero mesons, this singularity actually decouples, and the leading J-plane singularity is at $J=-2$.

ACKNOWLEDGMENTS

This work was supported by the Department of Energy under Contract No. DE-AC03-76SF00515. The work of G.P.L. was supported by the National Science Foundation.

[1]G. P. Lepage and S. J. Brodsky, Phys. Rev. D 22, 2157 (1980); Phys. Lett. 87B, 359 (1979); S. J. Brodsky and G. P. Lepage, in *Quantum Chromodynamics,* proceedings of the 1978 La Jolla Institute Summer Workshop, edited by W. Frazer and F. Henyey (AIP, New York, 1979); G. P. Lepage and S. J. Brodsky, Phys. Rev. Lett. 43, 545 (1979); 43, 1625 (E) (1979); S. J. Brodsky and G. P. Lepage, in *Quantum Chromodynamics,* proceedings of the SLAC Summer Institute, 1979, edited by Anne Mosher (SLAC, Stanford, 1980); S. J. Brodsky, Y. Frishman. G. P. Lepage, and C. Sachradja, Phys. Lett. 91B, 239 (1980).

[2]G. R. Farrar and D. R. Jackson, Phys. Rev. Lett. 43, 246 (1979); V. L. Chernyak and A. R. Vhitnishii, Zh. Eksp. Teor. Fiz. Pis'ma Red. 25, 14 (1977) [JETP Lett. 25, 11 (1977)]; A. V. Efremov and A. V. Radyushkin, Dubna Reports Nos. JINR-E2-11535, 11983, and 12384 (unpublished), Riv. Nuovo Cimento 3, 1 (1980); Phys. Lett. 94B, 245 (1980); A. Duncan and A. H. Mueller, Phys. Rev. D 21, 1636 (1980); Phys. Lett. 90B, 159 (1980); M. K. Chase, Nucl. Phys. B167, 125 (1980).

[3]A report on this work is given by S. J. Brodsky and G. Lepage, Report No. SLAC-PUB-2587, presented to the XXth International Conference on High Energy Physics, Madison, Wisconsin, 1980 (unpublished); and in the Proceedings of the International Symposium on Multiparticle Dynamics, Brugge, Belgium, 1980 (unpublished). A general discussion of helicity selection rules in QCD is given by S. J. Brodsky and G. P. Lepage, in *High Energy Physics with Polarized Beams and Polarized Targets,* proceedings of the 1980 International Symposium, Lausanne, Switzerland, edited by C. Joseph and J. Soffer (Birkhauser, Basel, Switzerland and Boston, 1981); Phys. Rev. D (to be published).

[4]S. J. Brodsky and G. R. Farrar, Phys. Rev. Lett. 31, 1153 (1973); Phys. Rev. D 11, 1309 (1975); V. A. Matveev, R. M. Muradyan, and A. V. Tavkheldize, Lett. Nuovo Cimento 7, 719 (1973).

[5]For recent discussions of the Sudakov suppression of Landshoff singularities, see P. V. Landshoff and D. J. Pritchard, Z. Phys. C 6, C9 (1980); G. P. Lepage and S. J. Brodsky, Ref. 1; and A. H. Mueller, Columbia Report No. CU-TP-192 (unpublished). In the case of non-Abelian gauge theories, Mueller's analysis shows that pinch contributions are not completely suppressed in hadron-hadron scattering amplitudes, leading to a small power-law correction to the dimensional-counting prediction.

[6]Current data give $f_\pi \cong 93$ MeV, $f_K \cong 112$ MeV, $f_\rho \cong 154$ MeV, $f_\phi \cong 161$ MeV, and $f_\omega \cong 158$ MeV with uncertainties on the order of a few MeV.

[7]While this must be true for a π or ρ, it is not necessarily the case for a K whose quarks have very different masses. However, any significant asymmetry in $\phi_K(x,Q)$ would lead to a substantial enhancement of decays such as $\psi \to K^+K^-$ (relative to $\psi \to \pi^+\pi^-$). This seems inconsistent with experiments.

[8]K. Tsokos (in preparation). The singlet wave function is discussed by V. N. Baier and A. H. Grozin, Novosibirsk report, 1981 (unpublished); T. Ohrndorf, Report No. SI-80-1, University of Siegen, Germany, 1980 (unpublished). See also M. K. Chase, Ref. 2.

[9]This is equivalent to assuming that the quark distribution amplitude is independent of the meson's helicity. While plausible at low and moderate energies, this assumption is certainly incorrect for very large energies where (for four flavors)

$$\frac{\phi_{\rho\perp}(x,Q)}{\phi_{\rho L}(x,Q)} \to \left[\ln\frac{Q^2}{\Lambda^2}\right]^{-4/25}.$$

[10]M. A Shupe *et al.*, Phys. Rev. Lett. 40, 271 (1978); Phys. Rev. D 19, 1921 (1979).

[11]S. J. Brodsky, G. P. Lepage, and T. Huang, contribution to the XXth International Conference on High Energy Physics, Madison, 1980, Report No. SLAC-PUB-2540 (unpublished).

[12]For a complete analysis, see P. Damgaard (in preparation).

[13]R. Barbieri, E. D'Emilio, G. Curci, and E. Remiddi, Nucl. Phys. B154, 535 (1979). We note, however, that in principle there are higher-order corrections to this ratio from higher-particle Fock states of the η_c which couple to the hadronic decay channels but not $\gamma\gamma$.

[14]Such a singularity was anticipated before QCD. See M. J. Creutz, S. D. Drell, and E. A. Paschos, Phys. Rev. 178, 2300 (1969); S. J. Brodsky, F. F. Close, and J. F. Gunion, Phys. Rev. D 5, 138 (1972).

[15]*Note added in proof.* This calculation has now been completed by F. del Aguila and M. K. Chase, Oxford Report No. 54/81 (unpublished).